energies

MDPI

Article

Optimal Energy and Reserve Market Management in Renewable Microgrid-PEVs Parking Lot Systems: V2G, Demand Response and Sustainability Costs

Viviani Caroline Onishi [1,2,*], Carlos Henggeler Antunes [2,3] and João Pedro Fernandes Trovão [2,4]

1 Centre for Mechanical Technology and Automation, Department of Mechanical Engineering, Campus de Santiago, University of Aveiro, 3810-193 Aveiro, Portugal
2 INESC Coimbra, University of Coimbra, DEEC, Polo II, 3030-290 Coimbra, Portugal; ch@deec.uc.pt (C.H.A.); joao.trovao@usherbrooke.ca (J.P.F.T.)
3 Department of Electrical and Computer Engineering, University of Coimbra, Polo II, 3030-290 Coimbra, Portugal
4 Department of Electrical & Computer Engineering, University of Sherbrooke, Sherbrooke, QC J1K 2R1, Canada
* Correspondence: viviani@ua.pt

Received: 16 March 2020; Accepted: 8 April 2020; Published: 13 April 2020

Abstract: Vehicle-to-grid (V2G) technology heralds great promise as a demand-side resource to contribute to more efficient grid management and promote the use of decentralized renewable energy. In this light, we propose a new optimization model for the sustainable energy and reserve market management in renewable-driven microgrid (RMG) plug-in electric vehicles (PEVs) parking lot systems. The RMG is composed of a hybrid photovoltaic/wind/hydrogen energy and storage system, along with local dispatchable generation units and bidirectional grid connection. The RMG is coupled to a smart PEVs parking lot, which is equipped with grid-to-vehicle (G2V) and V2G technologies allowing for not only PEVs aggregation and control but also optimal allocation of energy resources. Time-of-use (TOU) prices are considered in a demand response program (DRP) to enhance both economic and environmental performances by encouraging end-users to shift their energy demands from peak to off-peak time periods. Additionally, the model accounts for an economic incentive to PEVs owners to compensate for battery degradation. The integrated system eco-efficiency is evaluated through the application of the novel life cycle assessment-based Eco-cost indicator. The resulting mixed-integer linear programming model to minimize sustainability costs is implemented in GAMS and solved to global optimality. Different case studies are performed to demonstrate the effectiveness of the proposed modelling approach. Energy analyses results reveal that the optimal G2V-V2G operation, allied to TOU prices in a DRP, and reserve market management can reduce around 42% the energy and environmental costs of the RMG-PEVs parking lot system.

Keywords: optimization; mixed-integer linear programming (MILP); plug-in electric vehicles (PEVs); smart parking lot (SPL); vehicle-to-grid (V2G); renewable energy; hydrogen storage system (HSS); demand response program (DRP); Eco-costs; eco-efficiency

1. Introduction

The global energy system is facing new challenges due to the need of decarbonizing the economy, the increasing penetration of renewable energy sources and the need of ensuring reliable and flexible energy services. Although the electrification of the transport sector may facilitate this energy transition, it will also constitute a significant burden to the power system in the near future. According to

the International Energy Agency (IEA), over 1 million new electric vehicles (EVs)—EVs comprise plug-in hybrid electric vehicles (PHEVs), battery electric vehicles (BEVs) and fuel-cell electric vehicles (FCEVs)—have been sold worldwide in 2017, which represents a growth of 54% in sales when compared to the previous year [1]. On-going supportive policies and cost reductions in EV-related technologies are expected to lead to considerable intensification in the market uptake of EVs in decades to come. To corroborate this trend, the multi-government Electric Vehicles Initiative (EVI) has set in motion the "EV30@30" campaign with the ambitious target of achieving 30% market share for EVs by 2030 for all EVI members [2]. The recently launched Transport Decarbonization Alliance (TDA) is also committed to galvanize the change in the transport sector towards the net-zero carbon emission (net-zero carbon emissions are achieved when the amount of anthropogenic carbon released is globally balanced with an equivalent amount of sequestered carbon over a specified period) mobility, by proposing feasible solutions to meet climate goals by 2050 [3].

The large-scale market uptake and diffusion of EVs will certainly provide important advantages to the sustainable development of economy and society, most of them associated with energy security improvement and environmental pollution mitigation. However, the widespread dissemination of EVs may also have adverse effects on the energy distribution system in terms of power quality, control and resiliency that could threaten the stability of energy services [4]. For instance, the uncoordinated charging of an escalating number of EVs may pose difficulties on the electric power grid such as peak loading, power losses, voltage and frequency deviations [5]. In addition, the intermittent and stochastic nature of renewable energy generation also hampers the optimal energy management and, consequently, the practical operation of renewable energy systems [6]. Hence, the broad penetration of EVs and fluctuating renewable resources into the energy matrix require the development of advanced management strategies to efficiently cope with matching energy demand and supply sides. Smart grid-related technologies, such as grid-to-vehicle (G2V) and vehicle-to-grid (V2G), can be implemented to surmount such issues, by allowing the bidirectional energy management through the smart charging/discharging of aggregated plug-in electric vehicles (PEVs) [7,8]. To do so, idle PEVs batteries are employed as energy storage devices that serve as an energy buffer for balancing energy supply to the grid [9,10].

1.1. Literature Review on V2G Optimization Approaches

The V2G concept was originally introduced by Kempton and Letendre [11] in the late 1990s, with the proposition of EVs as power resources to electricity utilities. In their pioneering work, the authors have demonstrated the benefits of peaking power and battery storage to electric power systems in a wide range of conditions. Notably, the authors have also anticipated that integrating EVs into power systems would facilitate large-scale penetration of intermittent renewable energy sources. Since then, the term "vehicle-to-grid" or "V2G" has been widely used to define the ability of PEVs—including battery electric vehicles (BEVs) and plug-in hybrid electric vehicles (PHEVs)—to communicate with the power grid for providing ancillary services such as peak shaving and frequency regulation [12–16].

The V2G technology can indeed offer several advantages to the power grid that include voltage support, energy demand shifting, increased electricity reliability, improved power quality, and solar and wind energy integration [17]. Nevertheless, the unpredictability of PEVs charging and discharging is particularly challenging for the optimal planning of power grid operations. As a result, V2G implementation is a demanding task that requires the application of cutting-edge optimization techniques to consider all constraints that must be satisfied in such complex energy scheduling problem [18,19], while trading-off objectives of distinct nature and energy supply and demand sides. A comprehensive review on scheduling methodologies and mathematical optimization approaches for the V2G implementation is provided in Ref. [20].

Ahmad and Sivasubramani [21] have addressed the grid-planning problem by using V2G operation to optimize the economic and emission dispatch in a radial distribution system. Even though the integration of renewable energy resources has not been considered by the authors, their results

demonstrate that the PEVs participation in the V2G market can enlarge about four-fold the fleet handling size of the existing power structure in comparison with the uncontrolled scenario. Nikoobakht et al. [22] have proposed a stochastic modelling approach for the optimal transmission operation of the coordinated integration of PEVs and renewable energy resources. Their results emphasize the importance of the V2G operation for alleviating the impact of the renewable energy variability on power system operations and reducing operating costs.

The optimal V2G operation by the aggregated charging/discharging scheduling of PEVs into smart parking lot (SPL) systems has attracted increased attention over the past few years, specially to mitigate the charging demand difficulties posed on the power grid. Honarmand et al. [23] have presented an optimization model for the PEVs scheduling into an SPL by incorporating the V2G technology and battery conditions such as the remaining battery capacity and age-of-battery (AOB). Honarmand et al. [24] have proposed a mixed-integer linear programming (MILP) model for the cost-effective scheduling of PEVs and renewable energy generation in an integrated microgrid-SPL system. Later, the same authors have developed a stochastic optimization approach for the PEVs charging and discharging self-scheduling in a solar photovoltaic-driven SPL [25]. Landi et al. [26] have also studied the optimization of PEVs charging/discharging scheduling in parking lots by taking advantage of the V2G operation. However, in addition to solving the PEVs scheduling problem, their mixed-integer nonlinear programming (MINLP) modelling approach is able to simultaneously optimize the SPL capacity and location. A related stochastic model has been pursued by Mortaz et al. [27] to determine the optimal investment planning for the V2G technology in a microgrid.

Since PEVs act as flexible load within renewable-driven microgrids (RMGs), they can take part in demand response programs (DRPs) to bring multiple benefits for system operators, PEVs owners and the upstream power grid [28]. Yet, the participation of PEVs in DRPs in the supply side has been largely overlooked to date. To surpass this limitation, Aliasghari et al. [28] have focused on solving the problem of the optimal scheduling of PEVs and RMGs in the energy day-ahead and reserve markets under demand response management. For achieving this goal, the authors have performed the cost minimization of a wind-driven microgrid equipped with a PEVs parking lot. Moreover, they have used a DRP based on time-of-use (TOU) prices to encourage end-users to reduce their energy consumption during the high price periods and/or shift demands to the low-price ones. Bagher Sadati et al. [29] have proposed a bi-level framework for the operational scheduling of a distribution system equipped with a PEVs parking lot and wind and solar energy sources. In their work, price-based and incentive-based DRPs have been used to maximize the distribution system profit. Whereas previous studies have provided insightful results, none of them have taken into consideration the effect of using additional renewable energy resources and/or hydrogen energy storage on the system flexibility and reliability. Furthermore, they have disregarded the optimization of the system eco-efficiency.

The eco-friendly aggregation and control of PEVs within an RMG context is a very complex endeavour. Besides dealing with different energy demands and available renewable energy technologies, the optimization task must also simultaneously consider the economic and environmental performances of the system. Within this framework, Shamshirband et al. [30] have developed a MINLP model for the optimal charging/discharging scheduling of PEVs aggregators in a smart microgrid equipped with V2G capability, through the minimization of operating costs and carbon emissions, though their study lacks the application of DRPs as an energy management strategy to improve system sustainability. Jannati and Nazarpour [31] have proposed a bi-objective framework for the optimization of renewable-driven SPL systems based on the weighted sum technique and a fuzzy decision-making algorithm. The authors have applied TOU prices in a DRP to minimize both operating costs and greenhouse gas (GHG) emissions, by shifting power demands from peak time periods to off-peak ones. Despite having considered several renewable and non-renewable energy resources in the SPL system, their model does not account neither for PEVs battery-related issues—e.g., AOB, use degradation and economic compensation, etc.—nor the participation of PEVs in energy and reserve markets.

1.2. Contributions of this New Approach

Altogether, the aforementioned difficulties motivate the question of how PEVs can be integrated into RMGs to improve energy services reliability and renewable shares. To address this important issue, we introduce a new optimization model for enhancing energy and reserve market management in RMG-PEVs parking lot systems (hereafter referred to as RMG-PEVs systems). Our economic-oriented modelling approach is developed upon a general RMG superstructure, which encompasses distinct renewable energy generation alternatives (photovoltaic, wind and hydrogen) and local dispatchable generation (LDG) units, along with hydrogen storage system (HSS) and bidirectional grid connection. Additionally, the RMG is coupled to a SPL that is equipped with both G2V and V2G technologies to allow improving the system flexibility through the optimal energy resources allocation. For tackling some demand management drawbacks in previous literature, we use both TOU prices in a DRP and PEVs reserve market participation to further increase the overall system reliability and flexibility by enhancing energy efficiency, demand response and distributed energy resources. The resulting MILP model is implemented in GAMS and solved to the global optimal solution that minimizes the sustainability costs objective function. Different case studies are carried out to demonstrate the effectiveness of the proposed model regarding the cost-effective and environmentally friendly RMG-PEVs system operation.

To overcome environmental-related shortcomings in preceding research, we evaluate the RMG-PEVs system eco-efficiency through the application of the novel life cycle assessment (LCA)-based Eco-cost indicator [32]. Eco-cost is a robust sustainability indicator of cradle-to-cradle LCA calculations within the circular economy that embraces the environmental costs of ecosystems, global warming, human health, and resources depletion. Thus, its application can be critical to maximize value for both system operator and end-user at minimum Eco-costs (environmental burden). To the best of our knowledge, although some attempts have been made to optimize both economic and emission dispatch [21,31], the application of the Eco-cost indicator has not been addressed in the pertaining literature so far. Additional major contributions and innovative features introduced by this study include:

(*i*) The development of an optimization approach encompassing economic and environmental RMG-PEVs system performances, which can be efficiently solved to global optimality by using state-of-the-art solvers.

(*ii*) The proposition of a more comprehensive superstructure including several renewable and non-renewable energy resources, hydrogen energy conversion and storage, G2V and V2G technologies, and the possibility of either purchasing or selling energy from/to the upstream power grid, as well as participating in the energy and reserve markets.

(*iii*) The consideration of an economic incentive to compensate for the battery degradation and further encourage the PEVs owners to participate in the energy and reserve markets.

The rest of this work is organized as follows. In Section 2, we present the proposed MILP modelling approach. The illustrative case studies used to demonstrate the accurateness of the new optimization model are described in Section 3. In Section 4, we report the main results obtained and discuss how the adopted energy management strategy can improve the decision-making process. Finally, we summarize the major remarks and conclusions, and outline some future research directions and opportunities to boost the practical implementation of integrated RMG-PEVs systems.

2. Mathematical Programming Model

The mathematical modelling approach for the optimal energy and reserve market management in RMG-PEVs systems is developed via a MILP formulation. The mathematical model is developed upon a comprehensive RMG-PEVs superstructure as shown in Figure 1. The RMG superstructure comprises a hybrid photovoltaic/wind/hydrogen energy generation system with hydrogen conversion and storage, LDG units for energy backup, and bidirectional grid connection. The RMG is connected to a smart PEVs

parking lot system equipped with both G2V and V2G technologies. The possibility of either purchasing or selling energy from/to the upstream power grid, and the PEVs participation in the energy and reserve markets are also considered in the RMG-PEVs superstructure. An economic-oriented optimization approach is proposed for the cost-effective and environmentally friendly system operation, in which the objective function accounts for the minimization of operating expenses and Eco-costs related to the energy consumption. Binary variables are used to represent the discrete decisions about the optimal PEVs charging/discharging profiles and on/off status of energy generation units in the RMG system. The model encompasses constraints for modelling the photovoltaic panels (PV), wind turbines (WTs), SPL, HSS, and LDG units, in addition to the global energy balance, and the schemes for energy reserve market and demand response management.

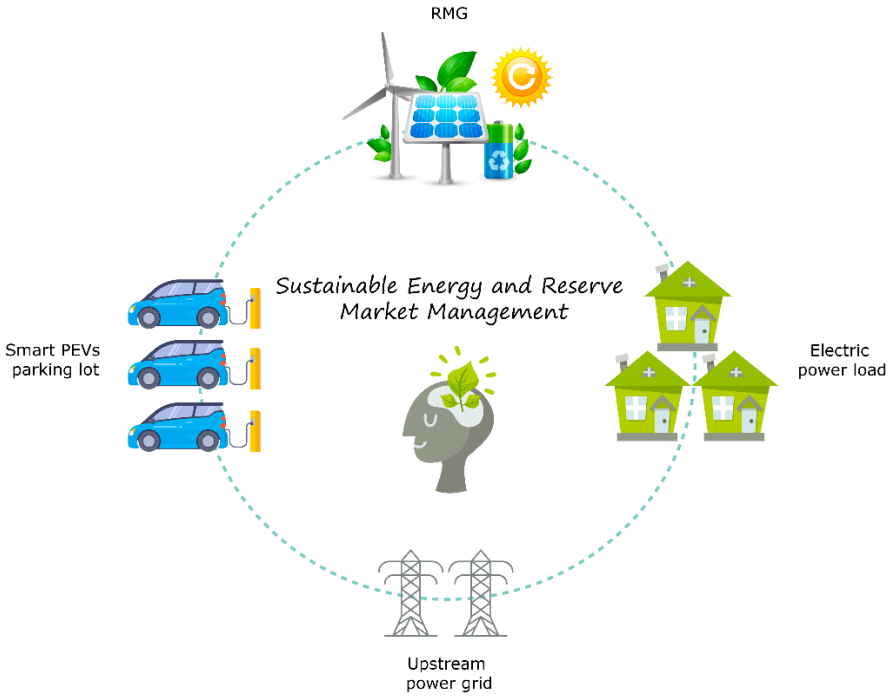

Figure 1. General superstructure for the sustainable energy and reserve market management in the renewable microgrid–plug-in electric vehicles parking lot (RMG-PEVs) system.

Let us first define the following index sets:

$$I = \{i/i = 1, \ldots, N_I \text{ is a PEV}\}$$
$$J = \left\{j/j = 1, \ldots, N_J \text{ is a LDG unit}\right\}$$
$$K = \{k/k = 1, \ldots, N_K \text{ is a WT}\}$$
$$T = \{t/t = 1, \ldots, N_T \text{ is a time period}\}$$

2.1. Photovoltaic Power System

The electric power output of the PV power system in each time step $t \in \{1, \ldots, N_T\}$ is obtained as a function of the hourly solar radiation flux (irradiance) G_t as follows [33].

$$P_t^{PV} = \eta_t^{PV} \cdot A^{PV} \cdot G_t \qquad \forall t \in T \tag{1}$$

In Equation (1), P_t^{PV} indicates the PV output power at instant $t \in T$ and A^{PV} the total area of the PV panels array. The efficiency of the PV panels η_t^{PV} is given by Equation (2).

$$\eta_t^{PV} = \eta^{Ref} \cdot \eta^{PC} \left\{ 1 - \beta \left[T_t^{Amb} + G_t \left(\frac{T^{NOC} - 20}{800} \right) - T^{Ref} \right] \right\} \qquad \forall t \in T \tag{2}$$

η^{Ref} represents the reference module efficiency and η^{PC} the power efficiency (equal to 1 for a perfect maximum power tracker). T_t^{Amb} is the hourly ambient air temperature, while T^{NOC} and T^{Ref} refer to the nominal cell operating temperature usually specified by the manufacturer (in the case studies, a value of 43 °C is used as obtained from [33]), and the cell temperature at reference conditions (typically 25 °C), respectively. β is the temperature coefficient (set to 4.5×10^{-3} °C^1 for mono-Si with $\eta^{Ref} \simeq 0.12$ and $T^{Ref} \simeq 25$ °C [34]).

2.2. Wind Power System

The electric power output of each wind turbine $k \in \{1, \ldots, N_K\}$ in the time step $t \in \{1, \ldots, N_T\}$ is modelled in terms of the hourly forecasted wind speed S_t^{FW} as follows [28,35].

$$P_{k,t}^{WT} = \begin{cases} 0, & S_t^{FW} < S_k^{CI} \text{ or } S_t^{FW} \geq S_k^{CO} \\ \frac{S_t^{FW} - S_k^{CI}}{S_k^R - S_k^{CI}} \cdot P_k^R, & S_k^{CI} \leq S_t^{FW} < S_k^R \\ P_k^R, & S_k^R \leq S_t^{FW} < S_k^{CO} \end{cases} \qquad \forall k \in K,\ t \in T \tag{3}$$

In Equation (3), $P_{k,t}^{WT}$ and P_k^R are the output power and rated power of the wind turbine $k \in K$ in the time step $t \in T$, respectively. S_k^R indicates the rated wind speed, while the cut-in and cut-off wind speeds are represented by S_k^{CI} and S_k^{CO}, respectively.

2.3. Smart Plug-in Electric Vehicles Parking Lot System

As aforementioned, the RMG is coupled to a SPL to control and aggregate PEVs as a flexible load, which allows the excess of energy generation to be stored in their batteries for potential participation in energy and reserve markets. To do so, the SPL is equipped with both G2V and V2G technologies. The modelling constraints for the optimal SPL operation are adapted from references [23,24,31].

2.3.1. Constraints on Charging and Discharging Power

Let $x_{i,t}$ be the binary variable that designates the existence of the ith PEV in the SPL in the time step $t \in \{1, \ldots, N_T\}$, while $y_{i,t}^{G2V}$ and $y_{i,t}^{V2G}$ are the binary variables that indicate the charging (G2V) and discharging (V2G) modes of each PEV $i \in \{1, \ldots, N_I\}$ in the same period, respectively:

$$\begin{aligned} x_{i,t} &= \begin{cases} 1 & \textit{if the PEV } i \textit{ is in the SPL in the time period } t \\ 0 & \textit{otherwise} \end{cases} \\ y_{i,t}^{G2V} &= \begin{cases} 1 & \textit{if the PEV } i \textit{ is in charging mode in the time period } t \\ 0 & \textit{otherwise} \end{cases} \\ y_{i,t}^{V2G} &= \begin{cases} 1 & \textit{if the PEV } i \textit{ is in discharging mode in the time period } t \\ 0 & \textit{otherwise} \end{cases} \\ \forall i \in I, &\quad t \in T \end{aligned}$$

The constraints on G2V and V2G modes are given by the following inequalities.

$$P_{i,t}^{G2V} \leq \overline{P}_i^{G2V} \cdot z_{i,t}^{G2V} \qquad \forall i \in I,\ t \in T \tag{4}$$

$$P_{i,t}^{V2G} \leq \overline{P}_i^{V2G} \cdot z_{i,t}^{V2G} \qquad \forall i \in I,\ t \in T \tag{5}$$

$P_{i,t}^{G2V}$ and $P_{i,t}^{V2G}$ are the decision variables regarding the amount of charging and discharging power of the ith PEV ($i \in I$) in the time step $t \in T$. $\overline{P}_i^{G2V}$ and $\overline{P}_i^{V2G}$ are the corresponding upper bounds parameters for the G2V and V2G electric power. In addition, $z_{i,t}^{G2V}$ and $z_{i,t}^{V2G}$ are integer variables used to linearize the discrete multiplications and $z_{i,t}^{V2G} = y_{i,t}^{V2G} \cdot x_{i,t}$ ($i \in \{1, \ldots, N_I\}$; $t \in \{1, \ldots, N_T\}$), as given by the following formulation.

$$\left.\begin{array}{l} z_{i,t}^{G2V} \le y_{i,t}^{G2V},\ z_{i,t}^{G2V} \le x_{i,t} \\ z_{i,t}^{V2G} \le y_{i,t}^{V2G},\ z_{i,t}^{V2G} \le x_{i,t} \\ y_{i,t}^{G2V} \ge y_{i,t}^{G2V} + x_{i,t} - 1 \\ z_{i,t}^{V2G} \ge y_{i,t}^{V2G} + x_{i,t} - 1 \end{array}\right\} \quad \forall\, i \in I,\ t \in T$$
$$z_{i,t}^{G2V},\ z_{i,t}^{V2G} \in \mathbb{Z} = [0,1];\ y_{i,t}^{G2V},\ y_{i,t}^{V2G},\ x_{i,t} \in \{0,1\} \qquad \forall\, i \in I,\ t \in T \tag{6}$$

2.3.2. Constraints on Charging and Discharging Modes of PEVs Battery

In each time period $t \in \{1, \ldots, N_T\}$, the electric power can be either purchased from or sold to the upstream power grid by the ith PEV ($i \in I$). The following inequality constraint is used to ensure that the G2V and V2G power modes are mutually exclusive.

$$y_{i,t}^{G2V} + y_{i,t}^{V2G} \le x_{i,t} \qquad \forall i \in I,\ t \in T \tag{7}$$

2.3.3. Constraints on SOC Levels of PEVs Battery

The SOC level of the ith PEV battery in the time step $t \in \{1, \ldots, N_T\}$, $SOC_{i,t}$, is obtained as follows.

$$\begin{array}{ll} SOC_{i,t} \cdot C_i = P_{i,t}^{G2V} \cdot \eta^{G2V} - P_{i,t}^{V2G} / \eta^{V2G} & \forall i \in I,\ t = 1 \\ SOC_{i,t} \cdot C_i = SOC_{i,t-1} \cdot C_i + P_{i,t}^{G2V} \cdot \eta^{G2V} - P_{i,t}^{V2G} / \eta^{V2G} & \forall i \in I,\ t > 1 \end{array} \tag{8}$$

In Equation (8), C_i represents the battery capacity of each PEV $i \in \{1, \ldots, N_I\}$. η^{G2V} and η^{V2G} are the PEVs battery charging and discharging efficiencies, respectively. The SOC level of PEVs battery ranges from the lower bound $\underline{SOC_i}$ to the upper bound $\overline{SOC_i}$ as given by constraint (9).

$$\underline{SOC_i} \le SOC_{i,t} \le \overline{SOC_i} \qquad \forall i \in I,\ t \in T \tag{9}$$

2.3.4. Constraints on Charging and Discharging Rates of PEVs Battery

The charging and discharging rates of the ith PEV ($i \in I$) battery in each time step $t \in \{1, \ldots, N_T\}$ is limited by the following constraint.

$$-\Delta SOC_i \le SOC_{i,t} - SOC_{i,t-1} \le \Delta SOC_i \qquad \forall i \in I,\ t \in T \tag{10}$$

In constraint (10), ΔSOC_i is the maximum charging/discharging rate allowed for each PEV battery.

2.3.5. Constraints on Departing SOC of PEVs Battery

Inequality constraints (11) and (12) are used to guarantee a desired battery SOC for each PEV $i \in \{1, \ldots, N_I\}$ at the departure time from the SPL.

$$SOC_{i,t} \ge SOC_i^{Arr} \qquad \forall i \in I,\ t \in T \tag{11}$$

$$SOC_i^{Dep} \ge SOC_i^{Arr} + \Delta SOC_i^{Req} \qquad \forall i \in I \tag{12}$$

SOC_i^{Arr} and SOC_i^{Dep} refer to the SOC of the ith PEV battery at the arriving to and departing from the SPL. ΔSOC_i^{Req} indicates the additional battery SOC required by each PEV $i \in \{1, \ldots, N_I\}$.

2.3.6. Constraints on the Maximum Number of G2V-V2G Modes Switches

The maximum number of switches $\overline{N}_i$ between charging (G2V) and discharging (V2G) modes, allowed for each PEV $i \in \{1, \ldots, N_I\}$ in the SPL, is determined according to the corresponding PEV's battery lifetime—also referred to as AOB [24]. Constraint (13) is used to restrict the number of switches between the G2V and V2G modes.

$$\sum_{t \in T} y_{i,t}^{G2V} + \sum_{t \in T} y_{i,t}^{V2G} \leq \overline{N}_i \qquad \forall i \in I \tag{13}$$

2.4. Energy and Reserve Market Management

We model the SPL as a virtual power plant within the RMG to provide electric power to the upstream grid through the PEVs participation in the energy and reserve markets as follows [28].

$$P_{i,t}^{V2G} = P_{i,t}^{V2G,sale} + P_{i,t}^{V2G,res} \qquad \forall i \in I,\ t \in T \tag{14}$$

$$P_{i,t}^{V2G,res} \leq C_i \cdot \left(SOC_{i,t} - \underline{SOC}_i\right) \qquad \forall i \in I,\ t \in T \tag{15}$$

$P_{i,t}^{V2G,sale}$ and $P_{i,t}^{V2G,res}$ are the discharging power of the PEV $i \in \{1, \ldots, N_I\}$ in the time step $t \in T$ for the energy and reserve market, respectively. The amount of electric power for the reserve market $P_{i,t}^{V2G,res}$ is restricted by constraint (15).

2.5. Upstream Power Grid Constraints

In the RMG-PEVs system, bidirectional grid connection is considered so that the electric power can be either purchased from (P_t^{grid}) or sold to (P_t^{sale}) the upstream power grid. The following constraints are used to ensure that the amount of electric power purchased from and sold to the upstream grid in the time period $t \in T$ do not exceed its capability (which is defined by the parameters $\overline{P}^{grid}$ and $\overline{P}^{sale}$).

$$P_t^{grid} \leq \overline{P}^{grid} \qquad \forall t \in T \tag{16}$$

$$P_t^{sale} \leq \overline{P}^{sale} \qquad \forall t \in T \tag{17}$$

2.6. Local Dispatchable Generators

Let $y_{j,t}^{LDG}$ be the binary variable that indicates the selection and on/off status of each LDG unit in the time step $t \in T$, in which,

$$y_{j,t}^{LDG} = \begin{cases} 1 & \textit{if the LDG unit } j \textit{ is used in the time period } t \\ 0 & \textit{otherwise} \end{cases}$$
$$\forall j \in J,\ t \in T$$

The electric power output of each LDG unit $j \in \left\{1, \ldots, N_J\right\}$ in the time step $t \in \{1, \ldots, N_T\}$ is limited by the following constraints [24].

$$\begin{aligned} P_{j,t}^{LDG} &\leq \overline{P}_j^{LDG} \cdot y_{j,t}^{LDG} \qquad \forall j \in J,\ t \in T \\ P_{j,t}^{LDG} &\geq \underline{P}_j^{LDG} \cdot y_{j,t}^{LDG} \qquad \forall j \in J,\ t \in T \end{aligned} \tag{18}$$

In Equation (18), $\overline{P}_j^{LDG}$ and $\underline{P}_j^{LDG}$ are the upper and lower bounds, respectively, for the electric power of the jth LDG unit. The ramp up and ramp down restrictions for the LDG units are given by constraint (19) [25,31].

$$\begin{array}{ll} P_{j,t}^{LDG} - P_{j,t-1}^{LDG} \le R_j^{UP} \cdot y_{j,t}^{LDG} & \forall j \in J,\ t \in T \\ P_{j,t-1}^{LDG} - P_{j,t}^{LDG} \le R_j^{DOWN} \cdot y_{j,t-1}^{LDG} & \forall j \in J,\ t \in T \end{array} \tag{19}$$

R_j^{UP} and R_j^{DOWN} are the ramp up and down rates of each LDG unit. In addition, the minimum up and down time constraints are expressed as follows [24].

$$\begin{array}{ll} y_{j,t}^{LDG} - y_{j,t-1}^{LDG} \le y_{j,t+UP_j}^{LDG} & \forall j \in J,\ t \in T \\ y_{j,t-1}^{LDG} - y_{j,t}^{LDG} \le 1 - y_{j,t+DN_j}^{LDG} & \forall j \in J,\ t \in T \\ UP_j = \begin{cases} t_j^{ON/OFF} & t_j^{ON/OFF} \le MUT_j \\ 0 & t_j^{ON/OFF} > MUT_j \end{cases} & \forall j \in J \\ DN_j = \begin{cases} t_j^{ON/OFF} & t_j^{ON/OFF} \le MDT_j \\ 0 & t_j^{ON/OFF} > MDT_j \end{cases} & \forall j \in J \end{array} \tag{20}$$

In Equation (20), UP_j and DN_j represent the minimum up and down time constraints, respectively, for each LDG unit $j \in J$. $t_j^{ON/OFF}$ is the minimum on/off time coefficient that corresponds to the time period in which the jth LDG unit is maintained continuously up or down. MUT_j and MDT_j are the limits for the minimum up and down times for the jth LDG unit, respectively.

2.7. Hydrogen Storage System

The amount of energy stored in the hydrogen tank of the HSS in each time step $t \in \{1, \ldots, N_T\}$ corresponds to the hydrogen production by the electrolyzer, $H2_t^{EL}$, via energy consumption in off-peak periods, which is given by Equation (21) [31,33].

$$\begin{array}{ll} H2_t^{EL} = \left(P_t^{EL} - P_t^{FC}/\eta^{C/I}\right) \cdot \eta^{EL} & \forall t = 1 \\ H2_t^{EL} = H2_{t-1}^{EL} + \left(P_t^{EL} - P_t^{FC}/\eta^{C/I}\right) \cdot \eta^{EL} & \forall t > 1 \end{array} \tag{21}$$

The amount of energy produced by the fuel cell in the time step $t \in \{1, \ldots, N_T\}$, $H2_t^{FC}$, through the hydrogen consumption in peak periods is stated in (22).

$$\begin{array}{ll} H2_t^{FC} = \left(P_t^{FC}/\eta^{C/I} - P_t^{EL}\right)/\eta^{FC} & \forall t = 1 \\ H2_t^{FC} = H2_{t-1}^{FC} - \left(P_t^{FC}/\eta^{C/I} - P_t^{EL}\right)/\eta^{FC} & \forall t > 1 \end{array} \tag{22}$$

In Equation (21) and Equation (22), P_t^{EL} and P_t^{FC} represent the electric power requested by the electrolyzer and the electric power supplied by the fuel cell, respectively, in the time step $t \in \{1, \ldots, N_T\}$. η^{EL} and η^{FC} are the electrolyzer and fuel cell efficiencies, respectively. $\eta^{C/I}$ refers to the converter/inverter efficiency. Constraints (23)–(25) are required to limit the electric power requested/supplied by the electrolyzer/fuel cell in the time step $t \in T$.

$$\begin{array}{ll} P_t^{EL} \le \overline{P}^{EL} \cdot y_t^{EL} & \forall t \in T \\ P_t^{EL} \ge \underline{P}^{EL} \cdot y_t^{EL} & \forall t \in T \end{array} \tag{23}$$

$$\begin{array}{ll} P_t^{FC} \le \overline{P}^{FC} \cdot y_t^{FC} & \forall t \in T \\ P_t^{FC} \ge \underline{P}^{FC} \cdot y_t^{FC} & \forall t \in T \end{array} \tag{24}$$

$$y_t^{EL} + y_t^{FC} \le 1 \qquad \forall t \in T \tag{25}$$

$\overline{P}^{EL}$ and $\underline{P}^{EL}$ are the upper and lower bounds for the electrolyzer energy consumption, while $\overline{P}^{FC}$ and $\underline{P}^{FC}$ are the upper and lower limits for the fuel cell power production. y_t^{EL} and y_t^{FC} are binary variables that indicate the on/off status of the electrolyzer and fuel cell units in each time step $t \in T$. Constraint (25) is needed to ensure that the charging and discharging processes of the hydrogen tank are not simultaneous.

2.8. Demand Response Program

We use TOU prices in a DRP to optimize the RMG-PEVs system to encourage shifting some load demand from peak periods to off-peak periods. Thus, the electric power demand in the time step $t \in \{1, \ldots, N_T\}$ under the TOU prices in DRP, P_t^{load}, should be equal to the corresponding base load demand $P_{B_t}^{load}$ added to the amount of shifted load DRP_t [36].

$$P_t^{load} = P_{B_t}^{load} + DRP_t \qquad \forall t \in T \tag{26}$$

The decision variable DRP_t can be either positive or negative, which implies that the load can either increase or decrease in the time period $t \in T$. Clearly, the amount of shifted load should be lower than the base load demand in each time period. This is ensured by constraint (27).

$$|DRP_t| \leq \overline{DRP} \cdot P_{B_t}^{load} \qquad \forall t \in T \tag{27}$$

$\overline{DRP}$ is the upper bound for the shifted load. In this work, we consider that up to 20% of the base load can be shifted in the time step $t \in T$. In addition, the total balance of shifted load in all time periods (e.g., one day or 24 h) should be equal to zero, as given by (28).

$$\sum_{t \in T} DRP_t = 0 \tag{28}$$

Equation (28) guarantees that the base load throughout a reference time period is fixed and some amount of it is just transferred from the peak to the off-peak periods.

2.9. Energy Balance Constraint

In each time step $t \in \{1, \ldots, N_T\}$, all electric power demands (including the hourly RMG loads under TOU prices in a DRP and PEVs charging) should be met by the energy obtained through power generation (via PV panels, WTs and LDG units), storage (HSS), and/or purchasing (PEVs discharging and upstream power grid). For ensuring full coverage of electric power demands, the energy balance constraint (29) is included in the model.

$$P_t^{grid} + P_t^{PV} + \sum_{k \in K} P_{k,t}^{WT} + \sum_{j \in J} P_{j,t}^{LDG} + \sum_{i \in I} P_{i,t}^{V2G} + P_t^{FC} = P_t^{load} + \sum_{i \in I} P_{i,t}^{G2V} + P_t^{EL} + P_t^{sale} \qquad \forall t \in T \tag{29}$$

2.10. Objective Function: Sustainability Costs

The objective function of the proposed MILP model consists of the minimization of the total sustainability cost ($Cost^{Sust}$), which accounts for the contributions of the total operating costs and eco-costs related to energy consumption, as well as revenue from electricity sales. The objective function is formally expressed in (30).

$$\begin{aligned} \min \quad & Cost^{Sust} = \left(Cost^{OP} + Cost^{ECO}\right) - Revenue \\ s.t. \quad & Eq.(1) - Eq.(29) \end{aligned} \tag{30}$$

The total operating costs $Cost^{OP}$ include the start-up and operational expenses of the LDG units, as well as the electric power purchased from the upstream grid and PEVs via the V2G technology as given by Equation (31).

$$Cost^{OP} = \sum_{j\in J}\sum_{t\in T}\left(CSTU_{j,t}^{LDG} + C_{j,t}^{LDG}\right) + \sum_{t\in T} C_P{}_t^{EG} \cdot P_t^{grid} + \sum_{i\in I}\sum_{t\in T}\left(C_P{}^{V2G} \cdot P_{i,t}^{V2G}\right) \quad (31)$$

$CSTU_{j,t}^{LDG}$ and $C_{j,t}^{LDG}$ are the start-up and operational costs of the LDG units, respectively, as defined by the following constraints.

$$CSTU_{j,t}^{LDG} \geq \left(y_{j,t}^{LDG} - y_{j,t-1}^{LDG}\right) \cdot UDC_j \qquad \forall j \in J,\ t \in T \quad (31a)$$

$$C_{j,t}^{LDG} = a_j \cdot y_{j,t}^{LDG} + b_j \cdot P_{j,t}^{LDG} \qquad \forall j \in J,\ t \in T \quad (31b)$$

In Equation (31), $C_P{}_t^{EG}$ is the hourly electricity purchasing tariff, while $C_P{}^{V2G}$ is the cost parameter that works as an economic incentive for the PEVs owners to compensate for the battery degradation. This parameter plays an important role to make the participation in energy markets appealing for most of the PEVs owners, since the frequent charging/discharging cycles could reduce the batteries lifetime. In constraint (31a), UDC_j is the cost parameter for the start-up of each LDG unit $j \in J$. In Equation (31b), a_j and b_j are coefficients for the estimation of the operating cost of LDG units.

As mentioned before, we apply the novel eco-cost indicator [32] to enhance the eco-efficiency of the RMG-PEVs system. The eco-cost is a robust LCA-based indicator in the realm of circular economy that allows costing the environmental impacts through eco-cost coefficients. The latter comprise global warming, resources depletion, and environmental impacts on human health and ecosystems. In this work, the total eco-cost $Cost^{ECO}$ encompasses the environmental costs of the electricity consumed from the upstream grid and the energy usage by LDG units as stated by Equation (32).

$$Cost^{ECO} = \sum_{t\in T}\left(C_{ECO}^{EG} \cdot P_t^{grid} + \sum_{j\in J} C_{ECO}^{NG} \cdot P_{j,t}^{LDG}\right) \quad (32)$$

C_{ECO}^{EG} and C_{ECO}^{NG} are the corresponding eco-costs parameters as obtained from the Eco-costs/Value Ratio (EVR) model [32]. The total revenue includes the economic profits from the electricity sale for PEVs charging, sale of the electric power surplus to the upstream grid, and PEVs participation in the reserve market.

$$Revenue = \sum_{i\in I}\sum_{t\in T}\left(C_P{}^{G2V} \cdot P_{i,t}^{G2V}\right) + \sum_{t\in T}\left(C_P{}^{SG} \cdot P_t^{sale} + \sum_{i\in I} C_P{}^{V2G,res} \cdot P_{i,t}^{V2G,res}\right) \quad (33)$$

In Equation (33), $C_P{}^{G2V}$, $C_P{}^{SG}$ and $C_P{}^{V2G,res}$ are the cost parameters for the PEVs charging, electricity sale to the grid, and energy reserve market, respectively.

The developed MILP model was implemented in GAMS software [37] (version 26.1.0) and solved to global optimality through the deterministic global solver BARON [38], under the sub-solver CPLEX 12.7. A computer with an Intel® Core™ i5-3570M 3.40 GHz processor and 8 GB RAM running Windows 10 was used for solving the case studies.

3. Case Studies

Three different case studies were performed to verify the effectiveness of the proposed modelling approach for the optimal energy management and operation of the integrated RMG-PEVs system:

(*i*) Case study 1: RMG in the Energy Market

(*ii*) Case Study 2: RMG-PEVs Parking Lot System in the Energy and Reserve Markets

(*iii*) Case Study 3: RMG-PEVs Parking Lot System with Demand Response in the Energy and Reserve Markets

Figure 2 shows the hourly market energy prices and electricity load demands considered to solve the case studies. The solar radiation flux (irradiance) and ambient temperature data are presented in Figure 3, while the wind speed data assumed for solving the case studies are displayed in Figure 4. The previous forecasted weather data (including wind speed, solar radiance flux and ambient temperature) were based on real hourly information obtained from the Lisbon Weather Station (ILISBOAL20; N 38°43′44″, W 9°8′41″) for the same time period and location. The modelling parameters taken to optimize the PV solar and WTs power systems are exhibited in Table 1. Note that a total area of 2500 m^2 for the solar PV panels array and four WTs were considered in the system.

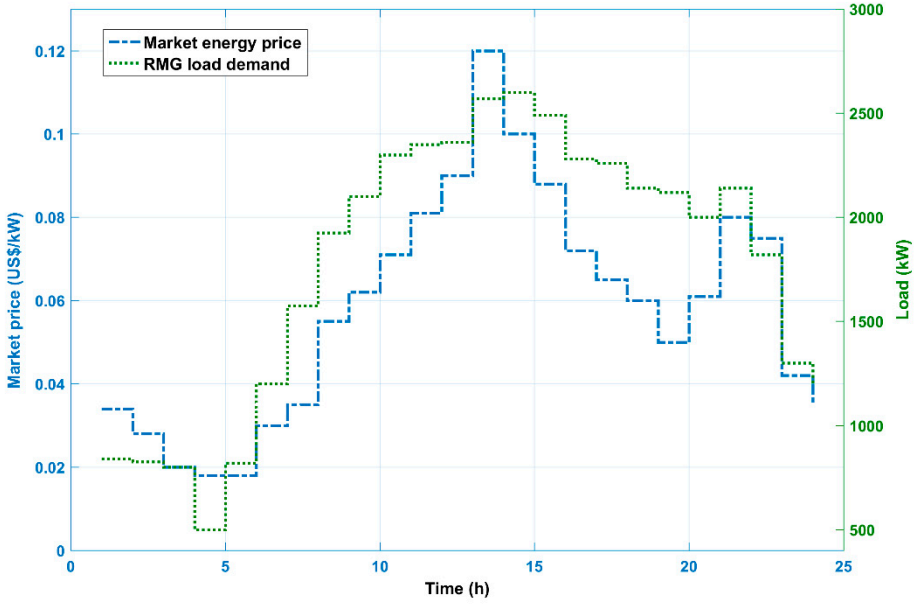

Figure 2. Hourly market energy prices and electricity load demands for the case studies.

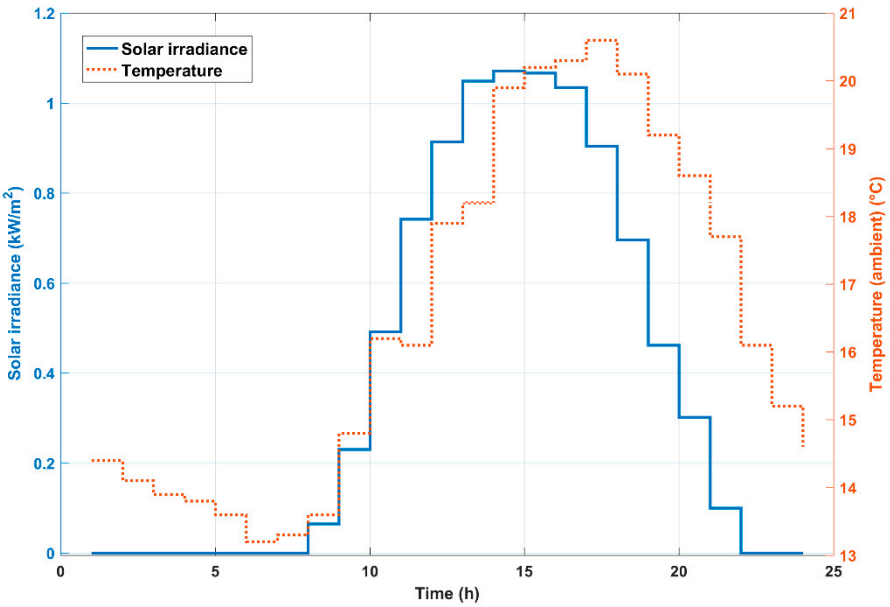

Figure 3. Solar radiation flux (irradiance) and ambient temperature data for the case studies.

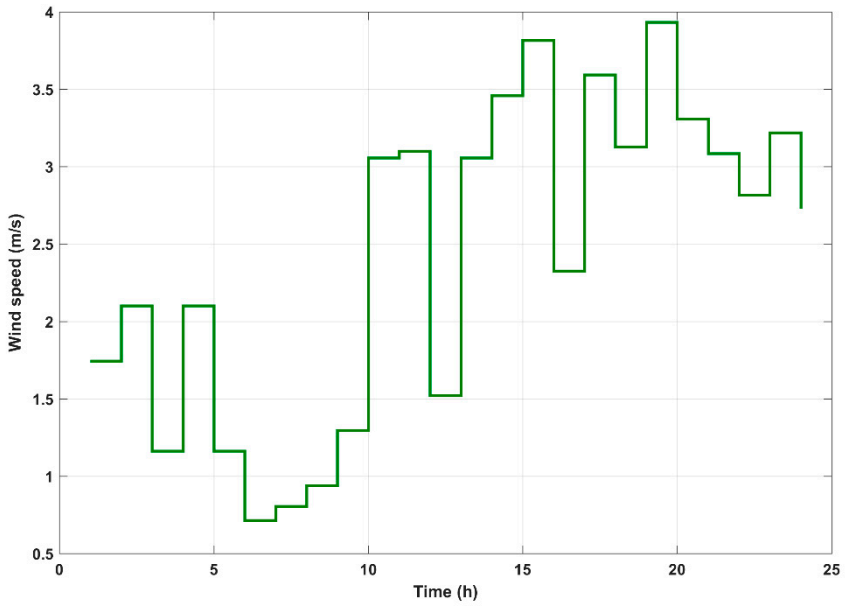

Figure 4. Wind speed data for the case studies.

Table 1. Modelling parameters for the renewable energy generation units [31,33,34].

Parameter	Symbol	Value (Unit)
PV power system		
Reference module efficiency	η^{Ref}	12 (%)
Nominal cell operating temperature	T^{NOC}	43 (°C)
Cell temperature at reference conditions	T^{Ref}	25 (°C)
Total area of the panels array	A^{PV}	2500 (m^2)
Temperature coefficient	β	0.0045 ($°C^{-1}$)
WT power system		
Rated power of wind turbines	P_k^R	500 (kW)
Rated wind speed	S_k^R	12 (m s^{-1})
Cut-in wind speed	S_k^{CI}	3 (m s^{-1})
Cut-out wind speed	S_k^{CO}	30 (m s^{-1})
Number of wind turbines	N_K	4 (-)

In all case studies, the maximum capacity of the smart parking lot was 100 PEVs. Additional modelling parameters for the smart PEVs parking lot are shown in Table 2. Although there currently are several PEVs brands in the market with different battery capacities, in this study we assume PEVs models with maximum battery capacities of 25 and 40 kWh [28]. However, these parameters can be easily changed in the model to account for different PEVs battery capacities. The arrival and departure times of the PEVs at/from the SPL system are random parameters in the model. Table 2 also shows the correlation between the number of switches between charging (G2V) and discharging (V2G) modes and the AOB, in which newer batteries (<4 years) present the highest number of allowed G2V-V2G mode switches. All modelling and cost parameters used for designing the LDG units and HSS system (including the electrolyzer, fuel cell, and converter/inverter) are given in Tables 3 and 4, respectively.

Table 2. Modelling parameters for the smart plug-in electric vehicles (PEVs) parking lot [23,24,28,31].

Parameter	Symbol	Value (Unit)
PEVs battery charging efficiency	η^{G2V}	90 (%)
PEVs battery discharging efficiency	η^{V2G}	80 (%)
Maximum charging power	$\overline{P}_i^{G2V}$	25–40 (kWh)
Maximum discharging power	$\overline{P}_i^{V2G}$	25–40 (kWh)
SOC level of batteries	$SOC_{i,t}$	0–100 (%)
Maximum charging/discharging rate	ΔSOC_i	80 (%)
Arrival SOC level	SOC_i^{Arr}	20–70 (%)
Maximum number of mode switches	$\overline{N}_i$	4–8 (-)
Relation between the AOB and the maximum number of mode switches	**AOB [years]**	$\overline{N}_i$
	AOB < 4	8 (-)
	4 ≤ AOB < 6	6 (-)
	6 ≤ AOB ≤ 8	4 (-)

Table 3. Modelling and cost parameters for the local dispatchable generation (LDG) units [24,31].

Parameter	Symbol (Unit)	LDG Unit		
		MT-1	**MT-2**	**MT-3**
Minimum power production	$\underline{P}_j^{LDG}$ (kW)	150	100	50
Maximum power production	$\overline{P}_j^{LDG}$ (kW)	700	450	300
Ramp up power rate	R_j^{UP} (kW)	350	200	150
Ramp down power rate	R_j^{DOWN} (kW)	350	200	150
Minimum up time	MUT_j (h)	3	2	1
Minimum down time	MDT_j (h)	3	2	1
Minimum on/off time	$t_j^{ON/OFF}$ (h)	4	−6	−8
Start-up cost	UDC_j (US$)	0.10	0.020	0.020
Cost coefficient	a_j (US$)	0.034	0.032	0.030
Cost coefficient	b_j (US$)	0.065	0.067	0.070

Table 4. Modelling parameters for the hydrogen storage system (HSS) [31,33].

Parameter	Symbol	Value (Unit)
Electrolyser		
Nominal efficiency	η^{EL}	74 (%)
Minimum energy consumption	$\underline{P}^{EL}$	300 (kW)
Maximum energy consumption	$\overline{P}^{EL}$	1240 (kW)
Fuel cell		
Nominal efficiency	η^{FC}	50 (%)
Minimum electric power production	$\underline{P}^{FC}$	100 (kW)
Maximum electric power production	$\overline{P}^{FC}$	1200 (kW)
Converter/inverter		
Nominal efficiency	$\eta^{C/I}$	95 (%)

4. Results and Discussion

4.1. Case Study 1: RMG in the Energy Market

Firstly, we solved the model by considering only the RMG into the superstructure. Thus, the system was equipped with renewable energy generators—which included PV solar panels and WTs—LDG units for energy backup and the HSS (electrolyzer and fuel cell units) for hydrogen energy production

and storage. In addition, bidirectional grid connection was considered for allowing the RMG to participate in the energy market via either energy purchasing (when electricity tariffs are low) or selling (when energy selling tariffs compensate) from/to the upstream power grid in each time period. Figure 5 shows the hourly electric power output of the PV solar panels and WTs in the RMG. The optimal electric power dispatching results obtained in this case study are exhibited in Figure 6.

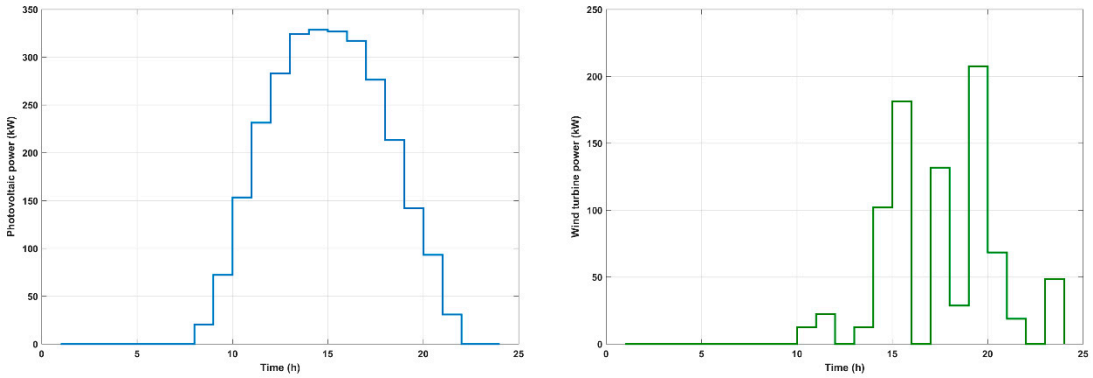

Figure 5. Power output of (**a**) photovoltaic solar panels and (**b**) wind turbines in the renewable microgrid–plug-in electric vehicles parking lot (RMG-PEVs) system.

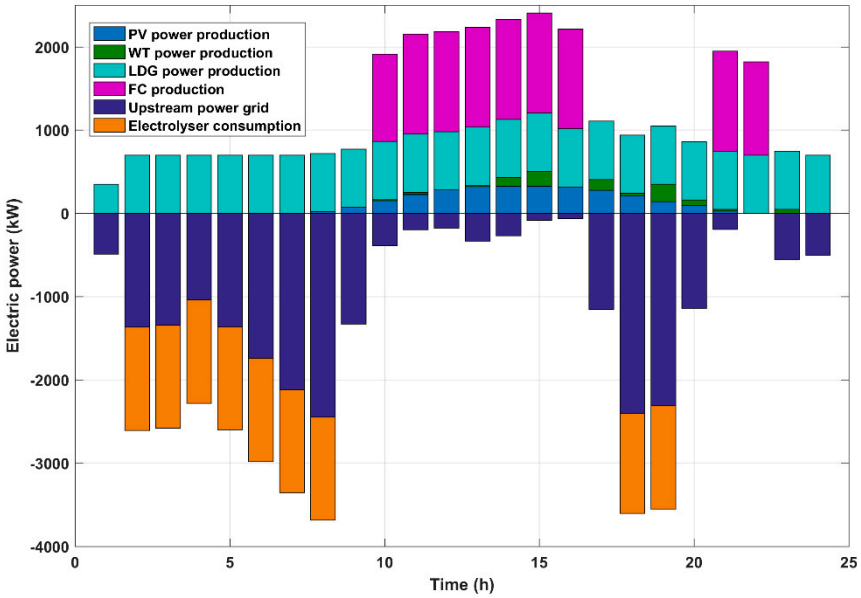

Figure 6. Optimal electric power dispatching results obtained in Case Study 1.

In this case, there was no surplus energy being produced in the RMG system so that no electricity was sold to the upstream power grid. Moreover, due to the higher electricity purchasing prices, considerably less energy was acquired from the grid between the time periods ranging from 10 to 16 h (see the hourly energy prices in Figure 2). For comparative purposes, consider, for instance, that the RMG required nearly 333 kW of electric power from the grid in time period 13, while ~2400 kW is needed in time period 18. In these time periods, the electricity prices were equal to US$0.12/kWh and US$0.06/kWh, respectively. It should be noted, however, that the periods comprised from 10 to 16 h also corresponded to the high energy load demand ones (see the hourly energy load demand in Figure 2). Hence, in these peak load periods, the RMG took advantage of the HSS by generating power via the hydrogen consumption through the fuel cell units. The hydrogen storage occurred in the off-peak periods (e.g., in the periods from 2 to 8 h), in which the energy prices were relatively lower.

In addition to the renewable energy generation, the LDG unit MT-1 operated at full capacity in almost all periods. Besides the minimum on/off time functioning requirements, this was an expected result since the LDG production expenses are generally lower than the purchasing electricity prices. The total sustainability cost for the optimal RMG scheduling was equal to US$5104, which was composed of US$2136 related to the operating expenditures—energy purchased from the upstream grid and start-up and fuel consumption by the MT-1 unit—and US$2968 associated with the Eco-costs of energy consumption. Since no electric power was sold to the grid, the RMG system had no revenues.

For evaluating the conditions that would allow the electricity to be sold by the RMG, we performed a parametric study regarding the energy selling prices. In this case, the electricity sale would only occur when the corresponding prices were higher than the peak purchasing tariff, i.e., when the selling prices were equal or higher than US$0.13/kWh. Alternatively, the electricity sale would take place if the Eco-costs were not considered in the objective function, whenever the energy selling prices were higher than the corresponding purchasing ones. Therefore, if the Eco-costs of energy consumption were not accounted to obtain the optimal solution, the system would buy much more electricity from the grid in the off-peak periods (where the purchasing prices are lower) to sell it in the peak ones. Under such a consideration, the total cost for the optimal RMG scheduling was equal to US$1689, which comprised US$2361 related to operating expenses and US$672 of revenue. Yet, the environmental impacts associated with the higher energy consumption would be much more expressive. In this particular case, the total Eco-costs were nearly 78% higher than the previous results in which they were minimized within the objective function. The latter results stress the importance of accounting for efficient economic and environmental metrics during the system scheduling to provide improved eco-efficiency performance solutions.

4.2. Case Study 2: RMG-PEVs Parking Lot System in the Energy and Reserve Markets

In this case study, we considered the RMG—hybrid photovoltaic/wind/hydrogen energy generation and storage system, non-renewable energy production by LDG units (as backup energy system) and bidirectional grid connection—coupled to the smart PEVs parking lot to appraise the potential benefits from the optimal aggregation of electric vehicles to the system. Note that, under this configuration, the RMG-PEVs system can take advantage of the energy storage in the PEVs' batteries, which is produced and/or acquired from the grid in the lower-price periods. In addition, the SPL was equipped with both G2V and V2G technologies for allowing the PEVs owners to participate in energy and reserve markets. The hourly electric power generated by the PV solar panels and WTs in the RMG-PEVs parking lot system is exhibited in Figure 5. The optimal electric power dispatching results obtained in this case study are depicted in Figure 7.

In addition to the renewable energy generation through the PV panels, WT units and fuel cell hydrogen consumption, the RMG-PEVs system required the operation of the LDG unit MT-1 in all periods (most of them in full capacity). As discussed before, this result was owed to the minimum on/off time functioning requirements of each LDG unit, and to the fact of their energy production costs being usually lower than the purchasing electricity tariffs. In this case, the system demanded a total of 29.23 MW from the upstream power grid for meeting energy loads, while 16.45 MW were produced through the LDG unit during the considered 24 h period. During this period, the total electricity purchasing expenses were nearly 13% higher than the LDG production costs. We also report that the electricity consumption from the grid was about 27% greater in comparison to the Case study 1. This is mainly due to the significant increase in load demands required by the optimal PEVs integration into the RMG. For instance, approximately 15% of the total energy load in time period 6 was related to the PEVs charging demand.

Like the previous case study, higher energy consumption from the grid was generally observed in periods in which purchasing prices were relatively lower (e.g., periods from 2 to 8 h; see the hourly energy prices in Figure 2), even if they presented lower load demands. Consequently, the periods ranging from 10 to 16 h presented lower power grid consumption. As they also corresponded to

the peak load periods, the system used the energy stored into the HSS throughout this time interval. A similar behaviour was also noticed in the periods 21 and 22. Note that, again, the hydrogen energy storage took place in the off-peak periods (e.g., in the periods from 2 to 8 h), in which the energy purchasing tariffs were lower. Furthermore, as a result of the Eco-costs minimization together with operating costs in the objective function, the RMG-PEVs system did not produce surplus energy for selling to the grid. However, the V2G capability allowed the broad PEVs participation in the energy and reserve markets. In fact, the energy storage into PEVs batteries during low-price periods improved considerably the flexibility and cost-efficiency of the system. As also shown in Figure 7, the PEVs battery storage allowed to further reduce the power grid consumption in peak load periods. In period 14, for instance, the amount of power required from the upstream grid was reduced from 269 to 0 kW, when compared to Case Study 1.

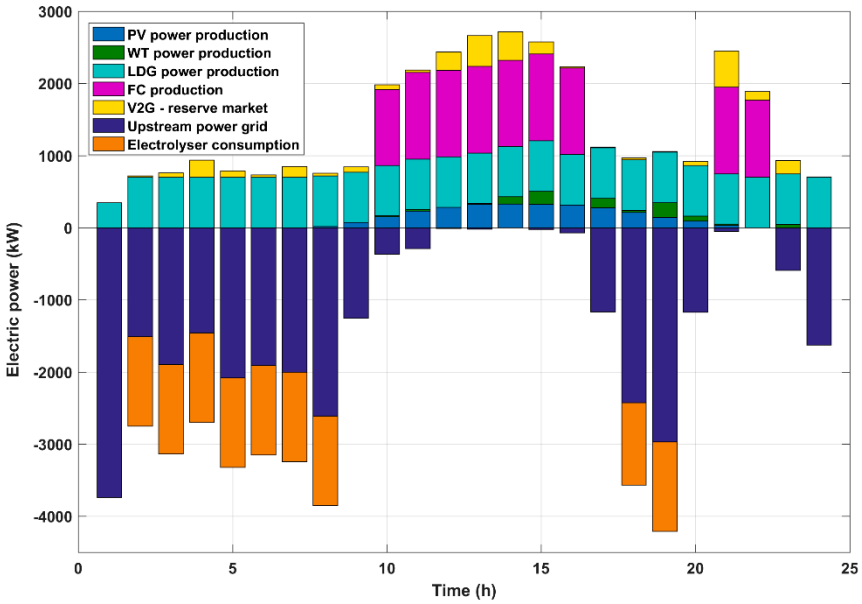

Figure 7. Optimal electric power dispatching results obtained in Case Study 2.

The total sustainability cost for the optimal energy and reserve market management of the RMG-PEVs parking lot system was equal to US$3108, in which US$3323 was related to operating expenses—i.e., energy purchased from the upstream grid and PEVs via the V2G technology, as well as start-up and fuel consumption by the MT-1 unit—and US$3607 was associated with the Eco-costs from the energy consumption. In this case, the RMG-PEVs system presented a total revenue of US$3822 obtained from the electricity sale for PEVs charging (G2V) and the PEVs participation in the reserve market. Hence, the optimal aggregation of PEVs into the RMG system allowed obtaining a reduction of ~39% in the total sustainability cost in contrast to the previous case study. Therefore, the decrease in the sustainability costs was mostly attributable to the revenues attained from the optimal PEVs integration in the RMG-PEVs system. We emphasize, nevertheless, that the escalation on both operational expenses (~56%) and Eco-costs (~22%) in comparison to Case 1 were indeed expected since the PEVs aggregation imposed a considerable burden to the RMG system, in terms of the amount of electric power required to meet their charging requirements.

4.3. Case Study 3: RMG-PEVs Parking Lot System with Demand Response in the Energy and Reserve Markets

Henceforth, we evaluated the effects of implementing TOU prices in a DRP on the optimal economic and environmental performances of the RMG-PEVs parking lot system. As with the previous case study, the system was composed of the RMG—hybrid PV/wind/hydrogen energy system, HSS, LDG units (as backup energy system) and bidirectional grid connection—linked to the smart PEVs

parking lot, which was equipped with both G2V and V2G technologies to allow the PEVs participation in energy and reserve markets. Since the same climate conditions were considered to optimize the problem, the hourly electric power output of the PV solar panels and WT units was consistent with that portrayed in Figure 5. However, the application of the TOU prices in a DRP promoted the shift in energy demand from peak to off-peak load periods. Figure 8 shows the hourly RMG load demands under TOU prices in a DRP found for Case Study 3. The optimal electric power dispatching results obtained in this case study are displayed in Figure 9.

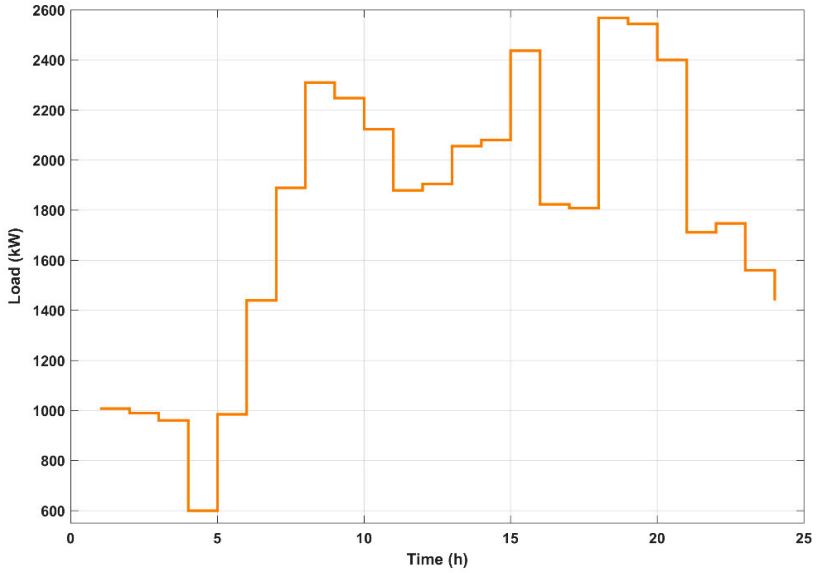

Figure 8. Hourly renewable microgrid load demands under time-of-use (TOU) prices in demand response program (DRP) obtained in Case Study 3.

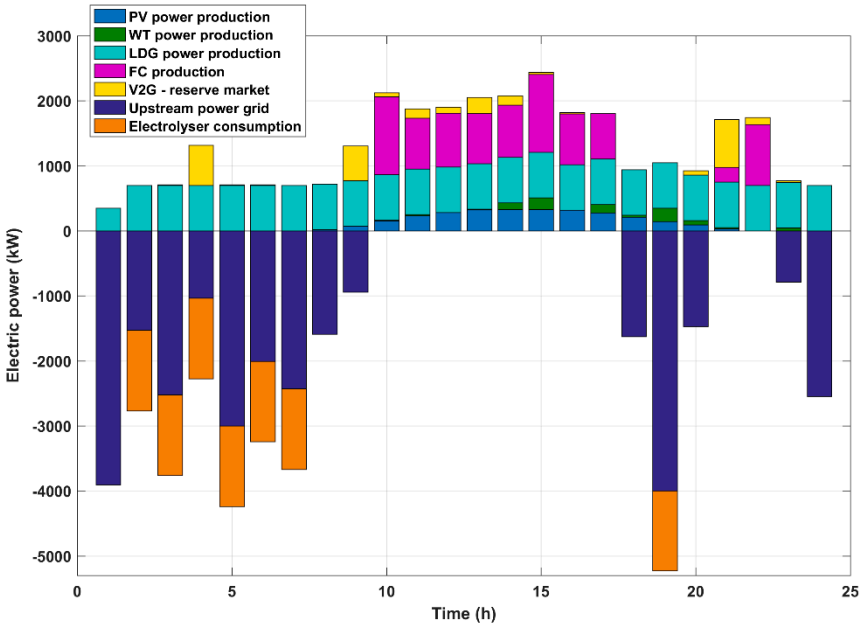

Figure 9. Optimal electric power dispatching results obtained in Case Study 3.

The optimal energy results obtained in this case study revealed that the implementation of the TOU prices in a DRP allowed the RMG-PEVs system to buy 0.6% more electric power from the upstream power grid, when compared to the previous case study. Furthermore, the system energy flexibility was significantly enhanced under the TOU scheme, since electricity was no longer acquired from the grid in

the peak load and price periods. Thus, no power was purchased from the grid in the periods ranging from 10 to 17 h, while 1.9 MW and 2.7 MW were required during this same time interval in Case 2 and Case 1, respectively. In addition, the purchase of electricity from the grid was not required in the periods 21 and 22 because of their higher energy prices despite the high load demand. We underline that in the peak periods from 10–17 h, as well as 21 and 22 h, the energy demands were met by the generated renewable energy (PV solar matrix and WTs) and the fuel cell hydrogen consumption. Then again, hydrogen energy is generally stored by the HSS during the off-peak periods (e.g., in the periods from 2 h to 7 h), which present comparatively lower purchasing tariffs.

In this case, the total sustainability cost for the optimal energy and reserve market management of the RMG-PEVs system was equal to US$2972, in which US$3170 was associated with the operating expenses—i.e., electricity acquired from the upstream power grid and PEVs discharging (V2G), and start-up and fuel consumption by the LDG unit MT-1—, and US$3623 was related to the Eco-costs from the energy consumption. We also report a total revenue of US$3821 achieved from the optimal PEVs charging (G2V) scheduling and participation in the reserve market. Hence, the implementation of the TOU prices in the system allowed us to reduce the total sustainability cost nearly 4.4% in comparison to the Case 2. As expected, this result is essentially attributed to the decrease of about 4.6% in the operating expenses. Note that the total Eco-costs obtained in Case 2 and Case 3 did not present significative difference, given that roughly the same total amount of electric power is required in both cases. Still, the RMG-PEVs system with DRP presented the total sustainability cost around 42% lesser than that estimated in Case 1. The later result is mainly owed to the considerable revenues obtained from the eco-friendly PEVs aggregation in the RMG system, which strongly emphasizes the advantages of the integrated G2V-V2G operation, together with the demand response program and optimal energy and reserve market management. Table 5 presents the optimal cost results obtained throughout the different case studies.

Table 5. Optimal costs obtained in the different case studies.

Case Study Description	Operating Costs (US$)	Eco-costs (US$)	Revenue (US$)	Total Sustainability Cost (US$)
1. RMG in the energy market	2136	2968	–	5104
2. RMG-PEVs in the energy and reserve markets	3323	3607	3822	3108
3. RMG-PEVs with TOU prices in a DRP in the energy and reserve markets	3170	3623	3821	2972

5. Conclusions

The growing penetration of renewable sources into the global energy matrix and the electrification of the transport sector constitute major challenges to the reliability and flexibility of energy services. As cornerstones of a decarbonized economy, renewable energy systems must effectively integrate electric vehicles to address these obstacles. In this light, we propose a new economic-oriented optimization model for improving sustainability in the energy and reserve market management of integrated RMG-PEVs systems. The modelling approach is developed upon a general superstructure including a hybrid PV solar panels/WTs/hydrogen energy and storage system, LDG units for energy backup, and bidirectional grid connection. The RMG is coupled to a SPL that is equipped with both G2V and V2G technologies to enhance the integrated RMG-PEVs system flexibility through the optimal energy resources allocation. The resulting MILP model is implemented in GAMS and solved to minimize overall sustainability costs. The capabilities of the proposed approach are evaluated through different case studies.

To the best of our knowledge, this is the first mathematical model for the cost-effective and environmentally friendly optimization of integrated RMG-PEVs systems to consider the novel LCA-based Eco-cost indicator for improving the system eco-efficiency. The major contributions from this work can be summarized as follows:

(*i*) The use of both TOU prices in a DRP and PEVs reserve market participation to further boost overall system reliability and flexibility by increasing energy efficiency, demand response and distributed energy resources.

(*ii*) The proposition of a MILP model encompassing the minimization of economic and environmental costs of integrated RMG-PEVs systems, which can be easily solved to the global optimal solution by using state-of-the-art optimization solvers.

(*iii*) The consideration of a more comprehensive system superstructure including several renewable and non-renewable energy resources, hydrogen energy conversion and storage, SPL with both G2V and V2G technologies, possibility of either purchasing or selling energy from/to the upstream power grid, and the PEVs participation in the energy and reserve markets.

(*iv*) The adoption of an economic incentive to compensate for the battery degradation and encourage the PEVs participation in the energy and reserve markets.

Regarding the main results obtained, we underline:

(*i*) The importance of considering both economic and environmental metrics during the system optimization to provide bettered eco-efficiency performance solutions. Note that the total Eco-costs are increased around 78% when they are not considered in the objective function.

(*ii*) The significance of developing integrated energy systems, which is highlighted by the reduction of nearly 39% in the total sustainability cost, when the PEVs smart parking lot is integrated into the RMG system (due to the increased revenues from electricity sales).

(*iii*) The impact of adopting advanced energy management alternatives, which is stressed by the decrease of around 42% in the total sustainability cost, when TOU prices in a DRP and PEVs reserve market participation, together with the G2V-V2G operation are also considered to optimize the RMG-PEVs system.

For these reasons, our optimization approach represents a useful tool for supporting decision-makers and planners towards the development and implementation of integrated RMG-PEVs systems. Future research will focus on developing the essential aspects related to the uncertain data (including weather data, energy demands and prices, etc.) and evaluating riskier decision-making attitudes.

Author Contributions: Conceptualization, V.C.O.; data curation, V.C.O.; methodology, V.C.O. and C.H.A.; formal analysis, V.C.O., C.H.A. and J.P.F.T.; resources and supervision, C.H.A.; writing—original draft preparation, V.C.O.; writing—review and editing, V.C.O., C.H.A. and J.P.F.T.; funding acquisition, V.C.O. and C.H.A. All authors have read and agreed to the published version of the manuscript.

Funding: This work was funded by the European Regional Development Fund through the COMPETE 2020 Programme, Portuguese Foundation for Science and Technology (FCT) and Regional Operational Program of the Center Region (CENTRO2020), through the projects SUSpENsE (CENTRO-01-0145-FEDER-000006), MAnAGER (POCI-01-0145-FEDER-028040), UIDB/00308/2020, CENTRO-01-0145-FEDER-022083, UIDB/00481/2020 and UIDP/00481/2020-FCT.

Conflicts of Interest: The authors declare no conflict of interest.

Nomenclature

Acronyms

AOB	Age-of-battery
BEV	Battery electric vehicle
DRP	Demand response program
EV	Electric vehicle
EVI	Electric Vehicles Initiative
EVR	Eco-costs/Value Ratio
FC	Fuel cell
FCEV	Fuel-cell electric vehicle

GAMS	General algebraic modelling system
GHG	Greenhouse gas
G2V	Grid-to-vehicle
HSS	Hydrogen storage system
IEA	International Energy Agency
LCA	Life cycle assessment
LDG	Local dispatchable generation
MINLP	Mixed-integer nonlinear programming
MILP	Mixed-integer linear programming
MT	Micro-turbine
PEV	Plug-in electric vehicle
PHEV	Plug-in hybrid electric vehicle
PV	Photovoltaic
RM	Renewable-driven microgrid
SOC	State-of-charge
SPL	Smart parking lot
TDA	Transport Decarbonization Alliance
TOU	Time-of-use
V2G	Vehicle-to-grid
WT	Wind turbine
Greek letters	
β	Temperature coefficient, $^{\circ}C^{-1}$
ΔSOC_i	Maximum charging/discharging rate
ΔSOC_i^{Req}	Additional state-of-charge level required by electric vehicles
$\eta^{C/I}$	Converter/inverter efficiency
η^{EL}	Electrolyser efficiency
η^{FC}	Fuel cell efficiency
η^{G2V}	Battery charging efficiency
η^{PC}	Power conditioning efficiency
η_t^{PV}	Efficiency of the photovoltaic panels
η^{Ref}	Reference module efficiency
η^{V2G}	Battery discharging efficiency
Roman letters	
a_j	Cost coefficient of local dispatchable generation units, US$
A^{PV}	Area of photovoltaic panels array, m^2
b_j	Cost coefficient of local dispatchable generation units, US$
C_i	Battery capacity, kW
$C_{j,t}^{LDG}$	Operating cost of local dispatchable generation units, US$
C_{ECO}^{EG}	Eco-cost parameter for the energy consumed from the power grid, US$ $(kWh)^{-1}$
C_{ECO}^{NG}	Eco-cost parameter for the energy produced by the local dispatchable generation units, US$ $(kWh)^{-1}$
$Cost^{ECO}$	Total eco-cost, US$
$Cost^{OP}$	Total operating cost, US$
$Cost^{Sust}$	Total sustainability cost, US$
$C_{P_t}^{EG}$	Electricity purchasing tariff, US$ $(kWh)^{-1}$
$C_P{}^{G2V}$	Cost parameter of electric vehicles charging, US$ $(kWh)^{-1}$
$C_P{}^{SG}$	Cost parameter of electric power sale to the grid, US$ $(kWh)^{-1}$
$C_P{}^{V2G}$	Cost parameter of electric vehicles discharging, US$ $(kWh)^{-1}$
$C_P{}^{V2G,res}$	Cost parameter of electric power sale to the energy reserve market, US$ $(kWh)^{-1}$
$CSTU_{j,t}^{LDG}$	Start-up cost of local dispatchable generation units, US$
DN_j	Minimum down time constraint of local dispatchable generation units, h
DRP_t	Shifted load demand, kW

G_t	Solar radiation flux, kW m^{-2}
$H_2{}_t^{EL}$	Hydrogen production by the electrolyzer, kW
$H_2{}_t^{FC}$	Hydrogen consumption by the fuel cell, kW
MDT_j	Minimum down time of local dispatchable generation units, h
MUT_j	Minimum up time of local dispatchable generation units, h
$\overline{N}_i$	Maximum number of switches between charging and discharging modes
P_t^{EL}	Energy consumption of the electrolyzer, kW
P_t^{FC}	Energy production of the fuel cell, kW
P_t^{grid}	Electric power purchased from the power grid, kW
$P_{i,t}^{G2V}$	Charging electric power, kW
$P_{j,t}^{LDG}$	Power production of local dispatchable generation units, kW
P_t^{load}	Electric power load demand under time-of-use of demand response program, kW
$P_{B_t}{}^{load}$	Base load demand, kW
P_t^{PV}	Power production of photovoltaic panels, kW
P_k^R	Rated power production of wind turbines, kW
P_t^{sale}	Electric power sold to the power grid, kW
$P_{i,t}^{V2G}$	Discharging electric power, kW
$P_{i,t}^{V2G,res}$	Discharging power for sale in the energy reserve market, kW
$P_{i,t}^{V2G,sale}$	Discharging power for sale in the energy market, kW
$P_{k,t}^{WT}$	Power production of wind turbines, kW
R_j^{DOWN}	Ramp down rate of local dispatchable generation units, kW
R_j^{UP}	Ramp up rate of local dispatchable generation units, kW
S_t^{FW}	Forecasted wind speed, m s^{-1}
S_k^{CI}	Cut-in wind speed, m s^{-1}
S_k^{CO}	Cut-off wind speed, m s^{-1}
S_k^R	Rated wind speed, m s^{-1}
$SOC_{i,t}$	State-of-charge level of electric vehicles
SOC_i^{Arr}	Arrival state-of-charge level
SOC_i^{Dep}	Departure state-of-charge level
T_t^{Amb}	Hourly ambient air temperature, °C
T^{NOC}	Nominal cell operating temperature, °C
$t_j^{ON/OFF}$	Minimum on/off time coefficient of local dispatchable generation units, h
T^{Ref}	Reference temperature, °C
UDC_j	Start-up cost parameter of local dispatchable generation units, US$
UP_j	Minimum up time constraint of local dispatchable generation units, h
$x_{i,t}$	Binary variable that takes the value «1» if a given electric vehicle is present in the parking lot
y_t^{EL}	Binary variable that takes the value «1» if the electrolyzer is used
y_t^{FC}	Binary variable that takes the value «1» if the fuel cell is used
$y_{i,t}^{G2V}$	Binary variable that takes the value «1» if a given electric vehicle is in charging mode in the parking lot
$y_{j,t}^{LDG}$	Binary variable that takes the value «1» if a given local dispatchable generation unit is used
$y_{i,t}^{V2G}$	Binary variable that takes the value «1» if a given electric vehicle is in discharging mode in the parking lot
$z_{i,t}^{G2V}$	Auxiliary integer variable that indicates the existence of electric vehicles and their charging mode
$z_{i,t}^{V2G}$	Auxiliary integer variable that indicates the existence of electric vehicles and their discharging mode
Subscripts	
i	Plug-in electric vehicle
j	Local dispatchable generation unit
k	Wind turbine
t	Time period

References

1. International Energy Agency (IEA). *Global EV Outlook 2018*; International Energy Agency: Paris, France, 2018.
2. International Energy Agency (IEA). *Global EV Outlook 2017: Two Million and Counting*; International Energy Agency: Paris, France, 2017.
3. Transport Decarbonisation Alliance (TDA). *Decarbonising Transport by 2050: A TDA Manifesto on How to Reach Net Zero Emission Mobility through Uniting Countries, Cities/Regions and Companies*; Transport Decarbonisation Alliance: Lisbon, Portugal, 2018.
4. Shaukat, N.; Khan, B.; Ali, S.M.; Mehmood, C.A.; Khan, J.; Farid, U.; Majid, M.; Anwar, S.M.; Jawad, M.; Ullah, Z. A survey on electric vehicle transportation within smart grid system. *Renew. Sustain. Energy Rev.* **2018**, *81*, 1329–1349. [CrossRef]
5. Lu, X.; Zhou, K.; Yang, S.; Liu, H. Multi-objective optimal load dispatch of microgrid with stochastic access of electric vehicles. *J. Clean. Prod.* **2018**, *195*, 187–199. [CrossRef]
6. Onishi, V.C.; Henggeler Antunes, C.; Gameiro, M.C. Smart and renewable energy systems: A critical overview on drivers, challenges and opportunities. In Proceedings of the 31st International Conference on Efficiency, Cost, Optimization, Simulation and Environmental Impact of Energy Systems, Guimarães, Portugal, 17–21 June 2018; pp. 1–9.
7. van der Kam, M.; van Sark, W. Smart charging of electric vehicles with photovoltaic power and vehicle-to-grid technology in a microgrid; a case study. *Appl. Energy* **2015**, *152*, 20–30. [CrossRef]
8. Modarresi Ghazvini, A.; Olamaei, J. Optimal sizing of autonomous hybrid PV system with considerations for V2G parking lot as controllable load based on a heuristic optimization algorithm. *Sol. Energy* **2019**, *184*, 30–39. [CrossRef]
9. Hu, X.; Wang, K.; Liu, X.; Sun, Y.; Li, P.; Guo, S. Energy Management for EV Charging in Software-Defined Green Vehicle-to-Grid Network. *IEEE Commun. Mag.* **2018**, *56*, 156–163. [CrossRef]
10. Mortaz, E.; Valenzuela, J. Optimizing the size of a V2G parking deck in a microgrid. *Int. J. Electr. Power Energy Syst.* **2018**, *97*, 28–39. [CrossRef]
11. Kempton, W.; Letendre, S.E. Electric vehicles as a new power source for electric utilities. *Transp. Res. Part D Transp. Environ.* **1997**, *2*, 157–175. [CrossRef]
12. Robledo, C.B.; Oldenbroek, V.; Abbruzzese, F.; van Wijk, A.J.M. Integrating a hydrogen fuel cell electric vehicle with vehicle-to-grid technology, photovoltaic power and a residential building. *Appl. Energy* **2018**, *215*, 615–629. [CrossRef]
13. Habib, S.; Kamran, M.; Rashid, U. Impact analysis of vehicle-to-grid technology and charging strategies of electric vehicles on distribution networks—A review. *J. Power Sources* **2015**, *277*, 205–214. [CrossRef]
14. Yong, J.Y.; Ramachandaramurthy, V.K.; Tan, K.M.; Mithulananthan, N. A review on the state-of-the-art technologies of electric vehicle, its impacts and prospects. *Renew. Sustain. Energy Rev.* **2015**, *49*, 365–385. [CrossRef]
15. Dogan, A.; Bahceci, S.; Daldaban, F.; Alci, M. Optimization of Charge/Discharge Coordination to Satisfy Network Requirements Using Heuristic Algorithms in Vehicle-to-Grid Concept. *Adv. Electr. Comput. Eng.* **2018**, *18*, 121–130. [CrossRef]
16. Kolawole, O.; Al-Anbagi, I. The impact of EV battery cycle life on charge-discharge optimization in a V2G environment. In Proceedings of the 2018 IEEE Power & Energy Society Innovative Smart Grid Technologies Conference (ISGT), Washington, DC, USA, 19–22 February 2018; pp. 1–5.
17. Noel, L.; Zarazua de Rubens, G.; Kester, J.; Sovacool, B.K. *Vehicle-to-Grid*; Springer International Publishing: Cham, Switzerland, 2019; ISBN 978-3-030-04863-1.
18. Tahanan, M.; van Ackooij, W.; Frangioni, A.; Lacalandra, F. Large-scale Unit Commitment under uncertainty. *4OR A Q. J. Oper. Res.* **2015**, *13*, 115–171. [CrossRef]
19. Ghotge, R.; Snow, Y.; Farahani, S.; Lukszo, Z.; van Wijk, A. Optimized scheduling of EV charging in solar parking lots for local peak reduction under EV demand uncertainty. *Energies* **2020**, *13*, 1275. [CrossRef]
20. Zheng, Y.; Niu, S.; Shang, Y.; Shao, Z.; Jian, L. Integrating plug-in electric vehicles into power grids: A comprehensive review on power interaction mode, scheduling methodology and mathematical foundation. *Renew. Sustain. Energy Rev.* **2019**, *112*, 424–439. [CrossRef]
21. Ahmad, M.S.; Sivasubramani, S. Optimal Number of Electric Vehicles for Existing Networks Considering Economic and Emission Dispatch. *IEEE Trans. Ind. Inform.* **2019**, *15*, 1926–1935. [CrossRef]

22. Nikoobakht, A.; Aghaei, J.; Khatami, R.; Mahboubi-Moghaddam, E.; Parvania, M. Stochastic flexible transmission operation for coordinated integration of plug-in electric vehicles and renewable energy sources. *Appl. Energy* **2019**, *238*, 225–238. [CrossRef]
23. Honarmand, M.; Zakariazadeh, A.; Jadid, S. Optimal scheduling of electric vehicles in an intelligent parking lot considering vehicle-to-grid concept and battery condition. *Energy* **2014**, *65*, 572–579. [CrossRef]
24. Honarmand, M.; Zakariazadeh, A.; Jadid, S. Integrated scheduling of renewable generation and electric vehicles parking lot in a smart microgrid. *Energy Convers. Manag.* **2014**, *86*, 745–755. [CrossRef]
25. Honarmand, M.; Zakariazadeh, A.; Jadid, S. Self-scheduling of electric vehicles in an intelligent parking lot using stochastic optimization. *J. Frankl. Inst.* **2015**, *352*, 449–467. [CrossRef]
26. Mohammadi Landi, M.; Mohammadi, M.; Rastegar, M. Simultaneous determination of optimal capacity and charging profile of plug-in electric vehicle parking lots in distribution systems. *Energy* **2018**, *158*, 504–511. [CrossRef]
27. Mortaz, E.; Vinel, A.; Dvorkin, Y. An optimization model for siting and sizing of vehicle-to-grid facilities in a microgrid. *Appl. Energy* **2019**, *242*, 1649–1660. [CrossRef]
28. Aliasghari, P.; Mohammadi-Ivatloo, B.; Alipour, M.; Abapour, M.; Zare, K. Optimal scheduling of plug-in electric vehicles and renewable micro-grid in energy and reserve markets considering demand response program. *J. Clean. Prod.* **2018**, *186*, 293–303. [CrossRef]
29. Bagher Sadati, S.M.; Moshtagh, J.; Shafie-khah, M.; Rastgou, A.; Catalão, J.P.S. Operational scheduling of a smart distribution system considering electric vehicles parking lot: A bi-level approach. *Int. J. Electr. Power Energy Syst.* **2019**, *105*, 159–178. [CrossRef]
30. Shamshirband, M.; Salehi, J.; Gazijahani, F.S. Decentralized trading of plug-in electric vehicle aggregation agents for optimal energy management of smart renewable penetrated microgrids with the aim of CO_2 emission reduction. *J. Clean. Prod.* **2018**, *200*, 622–640. [CrossRef]
31. Jannati, J.; Nazarpour, D. Optimal performance of electric vehicles parking lot considering environmental issue. *J. Clean. Prod.* **2019**, *206*, 1073–1088. [CrossRef]
32. The Model ofthe Eco-costs/Value Ratio (EVR). Delft University of Technology. Available online: http://www.ecocostsvalue.com (accessed on 10 November 2019).
33. Maleki, A.; Pourfayaz, F.; Ahmadi, M.H. Design of a cost-effective wind/photovoltaic/hydrogen energy system for supplying a desalination unit by a heuristic approach. *Sol. Energy* **2016**, *139*, 666–675. [CrossRef]
34. Skoplaki, E.; Palyvos, J.A. On the temperature dependence of photovoltaic module electrical performance: A review of efficiency/power correlations. *Sol. Energy* **2009**, *83*, 614–624. [CrossRef]
35. Ju, L.; Tan, Z.; Yuan, J.; Tan, Q.; Li, H.; Dong, F. A bi-level stochastic scheduling optimization model for a virtual power plant connected to a wind-photovoltaic-energy storage system considering the uncertainty and demand response. *Appl. Energy* **2016**, *171*, 184–199. [CrossRef]
36. Majidi, M.; Nojavan, S.; Zare, K. Optimal stochastic short-term thermal and electrical operation of fuel cell/photovoltaic/battery/grid hybrid energy system in the presence of demand response program. *Energy Convers. Manag.* **2017**, *144*, 132–142. [CrossRef]
37. Rosenthal, R.E. *GAMS—A User's Guide*; GAMS Development Corporation: Washington, DC, USA, 2016.
38. Tawarmalani, M.; Sahinidis, N.V. A polyhedral branch-and-cut approach to global optimization. *Math. Program.* **2005**, *103*, 225–249. [CrossRef]